

## Supplementary information

### Targeting cavity-creating p53 cancer mutations with small-molecule stabilizers: the Y220X paradigm

Matthias R. Bauer<sup>1‡</sup>, Andreas Krämer<sup>2,3‡</sup>, Giovanni Settanni<sup>4</sup>, Rhiannon N. Jones<sup>5</sup>, Xiaomin Ni<sup>2,3</sup>, Raysa Khan Tareque<sup>5</sup>, Alan R. Fersht<sup>1</sup>, John Spencer<sup>5</sup> & Andreas C. Joerger<sup>2,3\*</sup>

‡These authors contributed equally

\*Corresponding author: joerger@pharmchem.uni-frankfurt.de

<sup>1</sup> MRC Laboratory of Molecular Biology, Francis Crick Avenue, Cambridge Biomedical Campus, Cambridge CB2 0QH, UK.

<sup>2</sup> Institute of Pharmaceutical Chemistry, Johann Wolfgang Goethe University, Max-von-Laue-Str. 9, 60438, Frankfurt am Main, Germany.

<sup>3</sup> Buchmann Institute for Molecular Life Sciences and Structural Genomics Consortium (SGC), Max-von-Laue-Str. 15, 60438, Frankfurt am Main, Germany.

<sup>4</sup> Physics Department, Johannes Gutenberg University, Staudingerweg 7, 55099 Mainz, Germany

<sup>5</sup> Department of Chemistry, School of Life Sciences, University of Sussex, Falmer, Brighton, East Sussex BN1 9QJ, UK.

Table S1

Figures S1-S8

Supplemental references

**Table S1.** Average root-mean-square fluctuation across DBD residues 97-289

Codon 220 mutation <sup>1</sup>	Average RMSF (Å)	$T_m$ (°C)
<i>Native structure</i>		
WT	1.46	51.5
Y220H	1.56	45.1
Y220C	1.61	43.8
Y220N	1.64	39.9
Y220S	1.67	39.4
<i>Ligand complexes</i>		
Y220C-PK9323	1.35	
Y220S-PK9301	1.42	
Y220S-PK9323	1.58	

<sup>1</sup>MD simulations were performed in the framework of a stabilized quadruple mutant DBD (M133L/V203A/N239Y/N268D).

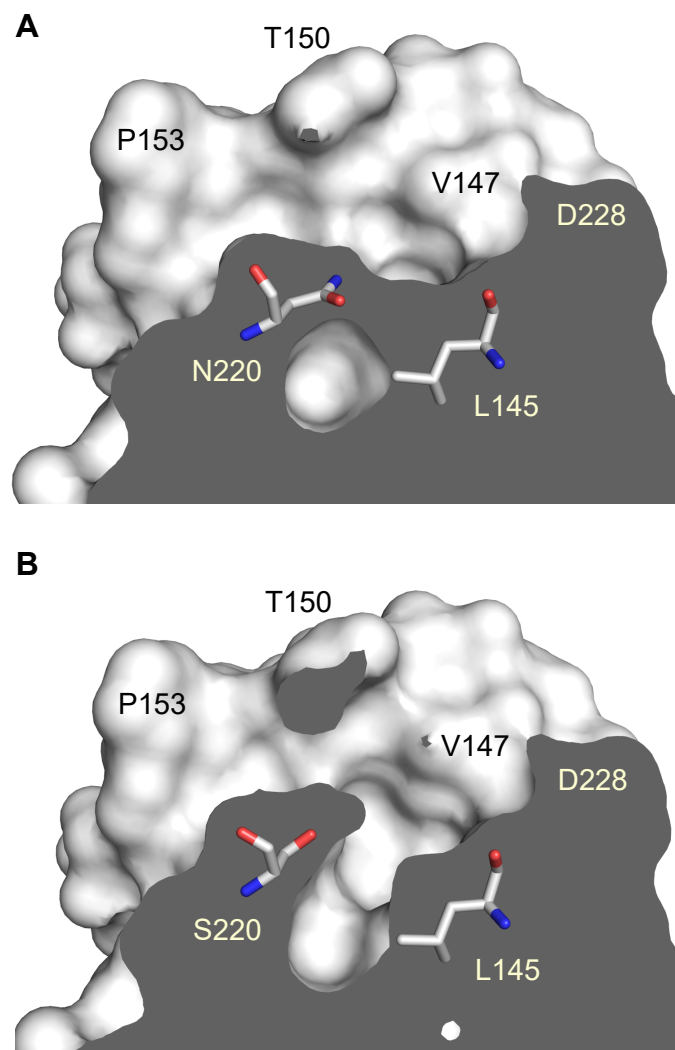


**Figure S1.** Structure of the p53 cancer mutant Y220N. Modelled surface crevice in mutant Y220N (A) showing a reduced depth at the center of the mutation-induced surface crevice compared with the crystal structure of the Y220S mutant (B). For both mutants, the same cross-section of the surface crevice is shown. The structure of the Y220N mutant was modelled with SWISS-MODEL<sup>1</sup> using PDB entry 2X0W as a template.

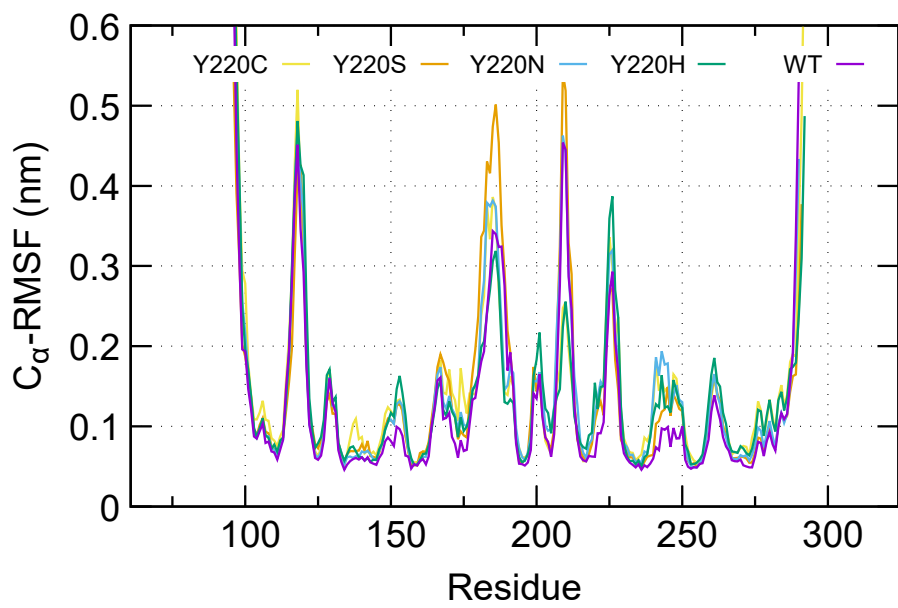


**Figure S2.** Root-mean-square fluctuation (RMSF) of C<sub>α</sub> atoms in MD simulations of the DBD of p53-Y220X mutants.

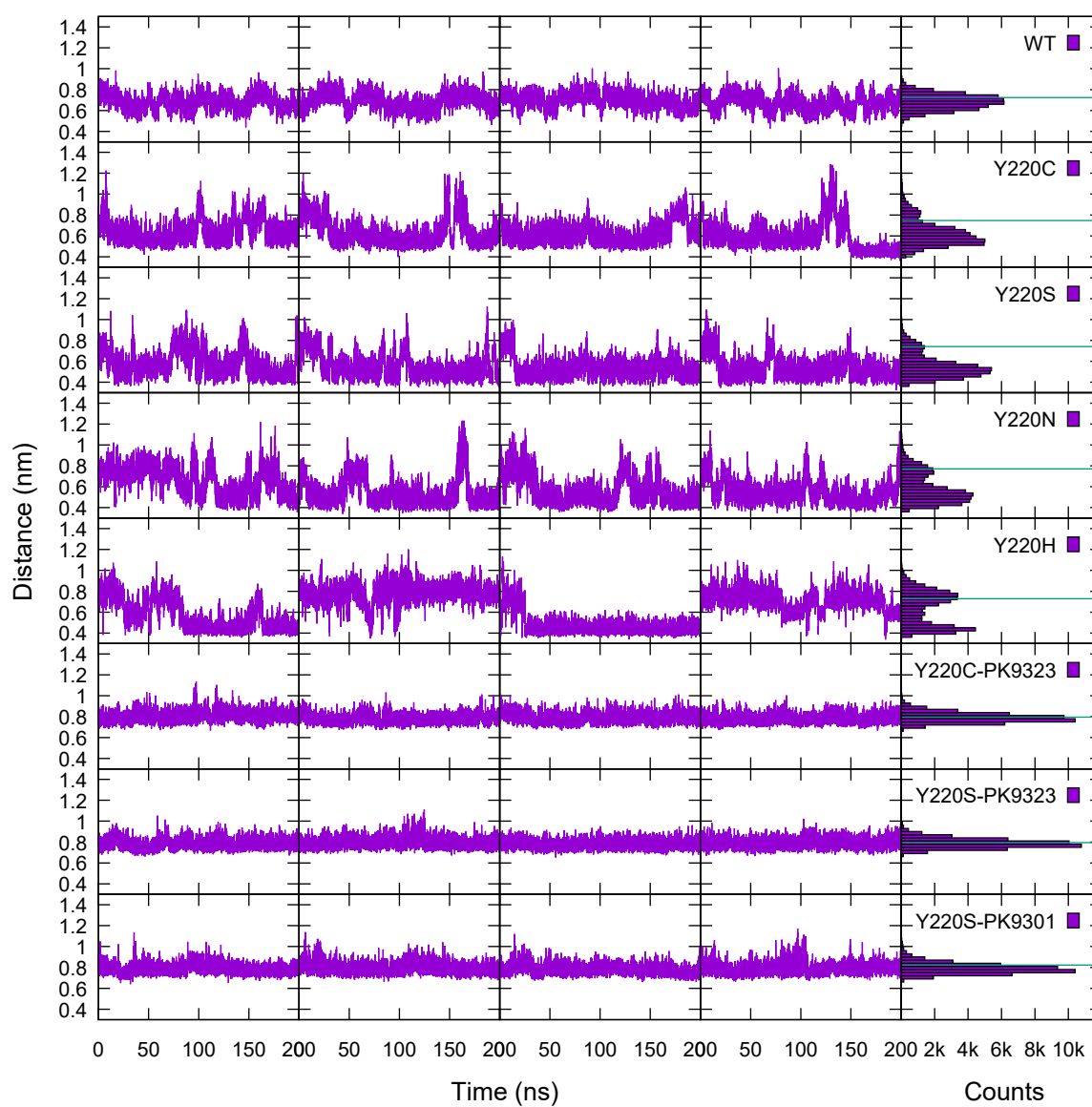


**Figure S3.** Distance between the  $C_{\delta}$  atoms of Pro151 and Pro223 as a function of time over all MD simulations. The green line indicates the distance in the corresponding crystal structures (chain A), or the starting model in case of the Y220N mutant.

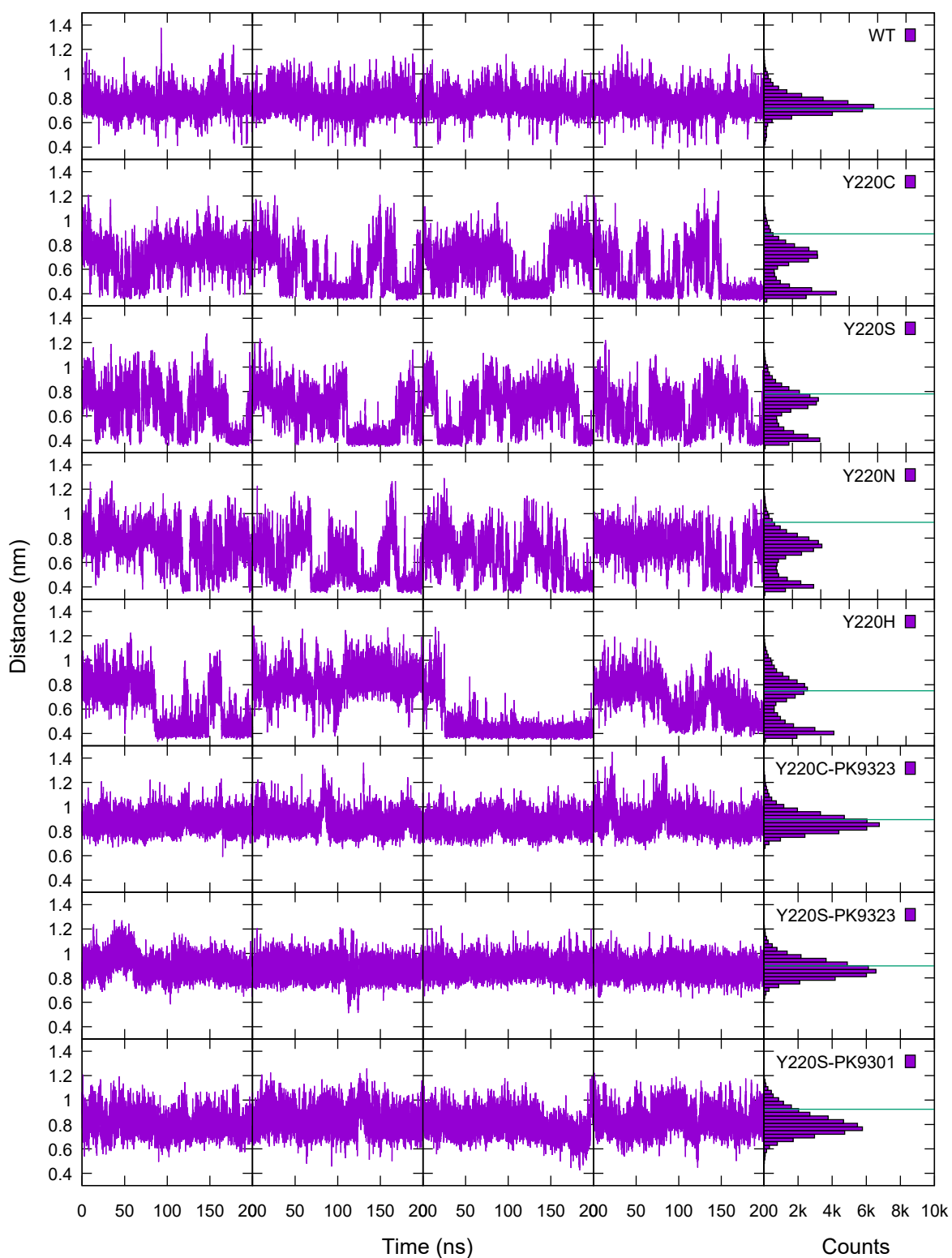


**Figure S4.** Distance between the  $C_{\alpha}$  atom of Pro153 and the  $C_{\gamma}$  atom Pro222 as a function of time over all MD simulations. The green line indicates the distance in the corresponding crystal structures (chain A), or the starting model in case of the Y220N mutant.

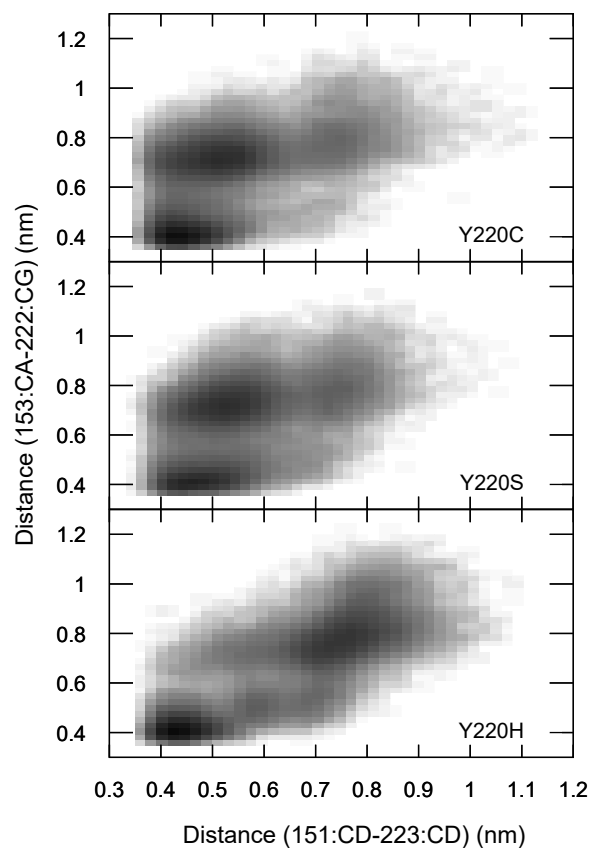


**Figure S5.** Correlation between subsite 2 and the central cavity in the MD simulations of the Y220S, Y220C and Y220H mutant. The correlation between the state of both subsites during the MD simulation was monitored by plotting the distance between the  $C_{\delta}$  atoms of Pro151 and Pro223 (d1; central cavity) versus the distance between the  $C_{\alpha}$  atom of Pro153 and the  $C_{\gamma}$  atom of Pro222 (d2; subsite 2).

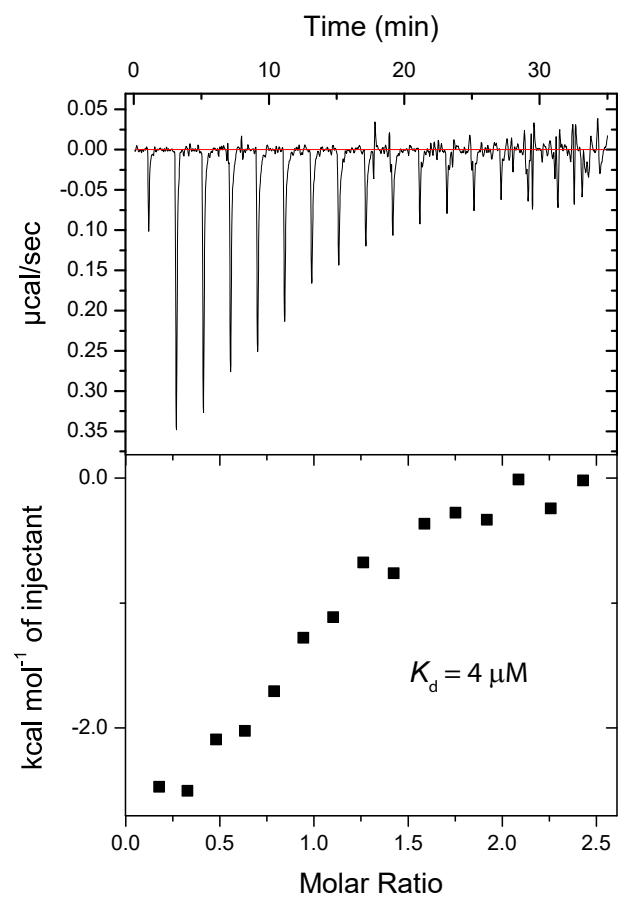


**Figure S6:** ITC curve for binding of PK9301 to p53 cancer mutant Y220S with resulting binding constant.



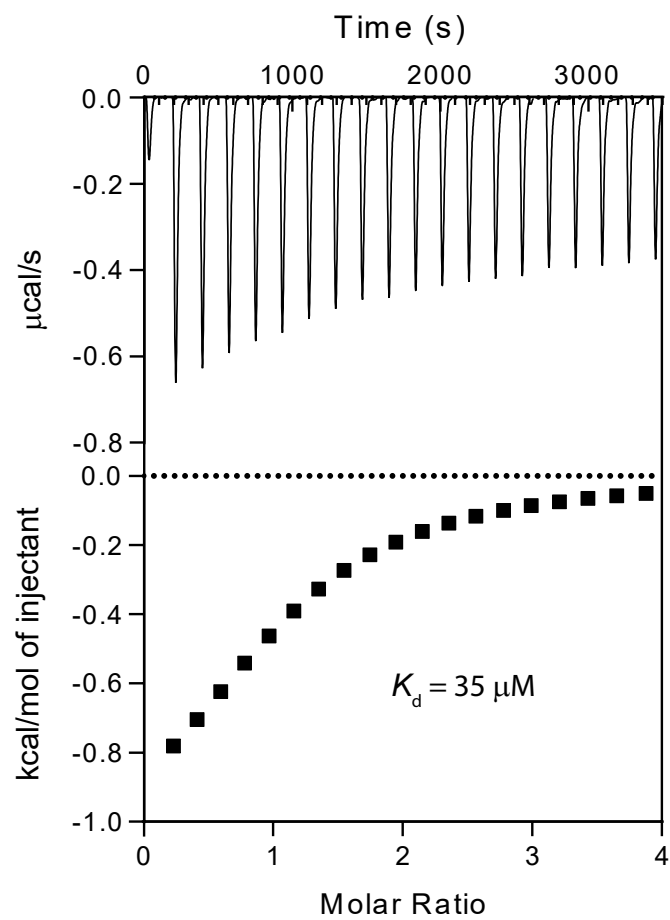


**Figure S7:** ITC curve for PK9255 binding to the p53 cancer mutant Y220N.

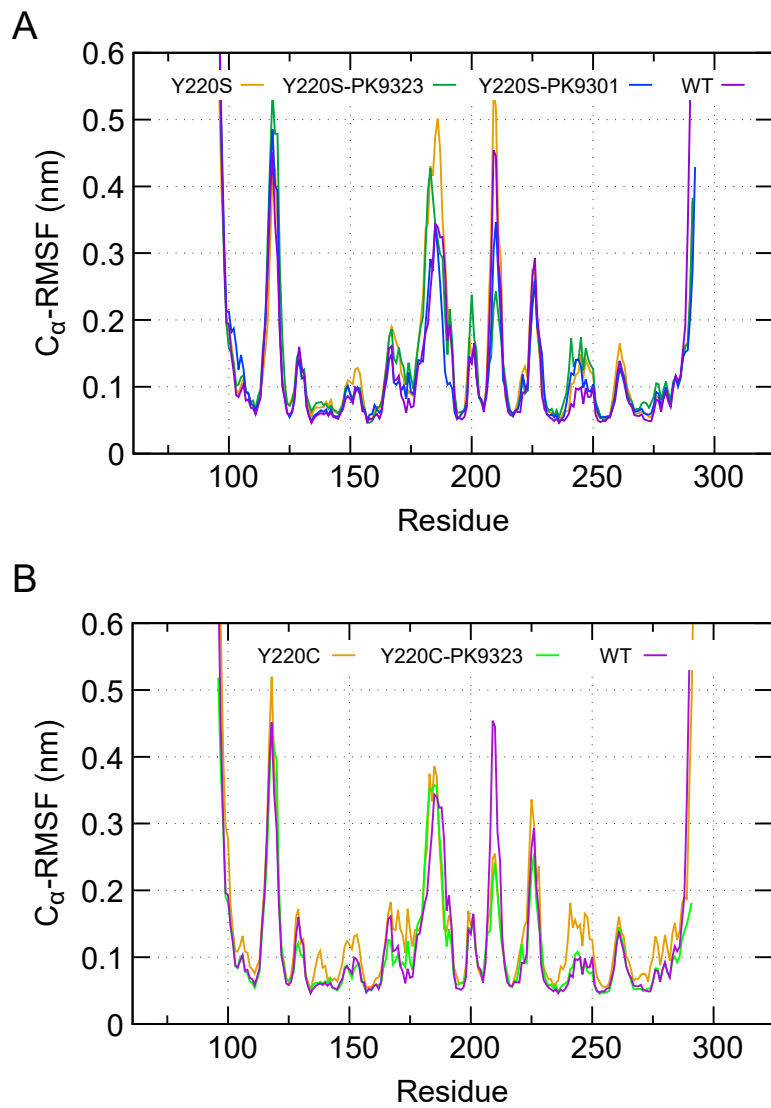


**Figure S8.** Root-mean-square fluctuation (RMSF) of C $\alpha$  atoms in MD simulations of p53-Y220X mutant DBDs. (A) Effect of ligand binding to the Y220S mutant. (B) Effect of ligand binding to the Y220C mutant.

## SI References

(1) Bienert, S., Waterhouse, A., de Beer, T. A., Tauriello, G., Studer, G., Bordoli, L., and Schwede, T. (2017) The SWISS-MODEL Repository-new features and functionality. *Nucleic Acids Res* 45, D313-D319.